Chemical Senses, 2023, **48**, 1–12
https://doi.org/10.1093/chemse/bjad001
Advance access publication 28 January 2023
Original Article

Original Article

Neural suppression in odor recognition memory

Tom Eek[1,2,3,*], Fredrik Lundin[1,2], Maria Larsson[4], Paul Hamilton[3,5], Charalampos Georgiopoulos[3,6,7,8]

[1]Department of Neurology, Linköping University, Linköping, Sweden
[2]Department of Biomedical and Clinical Sciences, Linköping University, Linköping, Sweden
[3]Center for Medical Image Science and Visualization, Linköping University, Linköping, Sweden
[4]Gösta Ekman Laboratories, Department of Psychology, Stockholm University, Stockholm, Sweden
[5]Center for Social and Affective Neuroscience, Department of Biomedical and Clinical Sciences, Linköping University, Linköping, Sweden
[6]Department of Radiology, Linköping University, Linköping, Sweden
[7]Department of Medical and Health Sciences, Linköping University, Linköping, Sweden
[8]Diagnostic Radiology, Department of Clinical Sciences, Medical Faculty, Lund University, Lund, Sweden

*Corresponding author: Department of Neurology, Linköping University Hospital, 581 85 Linköping, Sweden. Email: tom.eek@liu.se

Little is known about the neural basis of lower- and higher-order olfactory functions such as odor memory, compared with other sensory systems. The aim of this study was to explore neural networks and correlates associated with 3 functions: passive smelling (PS), odor encoding (OE), and in particular odor recognition memory (ORM). Twenty-six healthy participants were examined using functional magnetic resonance imaging conducted across 3 sessions, one for each function. Independent component analysis revealed a difference between sessions where a distinct ORM component incorporating hippocampus and posterior cingulate showed delayed triggering dissociated from odor stimulation and recognition. By contrasting Hit for ORM (target odors correctly recognized as old) and a combination of PS and detected odors from OE, we found significantly lower activations in amygdala, piriform cortex, insula, thalamus, and the inferior parietal lobule. Region of interest analysis including anterior insula, posterior cingulate gyrus, dentate gyrus, left middle frontal gyrus, amygdala, and piriform cortex demonstrated that Hit were associated with lower activations compared with other memory responses. In summary, our findings suggest that successful recognition of familiar odors (odor familiarity) is associated with neural suppression in the abovementioned regions of interest. Additionally, network including the hippocampus and posterior cingulate is engaged in a postrecognition process. This process may be related to incidental encoding of less familiar and more novel odors (odor novelty) and should be subject for future research.

Key words: episodic memory, olfaction, functional magnetic resonance imaging (fMRI), independent component analysis (ICA), region of interest analysis (ROI), familiarity

Introduction

In contrast to all other sensory inputs, olfactory information is transmitted first and foremost to brain regions subserving emotion, learning, and memory with no thalamic relay (Kim 2013; Zhou et al. 2021). Accordingly, behavioral evidence shows that episodic memory for odors differ from information processed by other sensory modalities (Engen and Ross 1973; Herz and Engen 1996; Arshamian et al. 2013; Cornell Kärnekull et al. 2015). For example, odor memories are typically experienced with a higher emotional intensity and show a slower forgetting function over time. Furthermore, olfactory cuing of autobiographical memory shows that evoked memories tend to cluster in childhood (<10 years of age) and accompanied by feelings of nostalgia and a sense of being brought back in time (Larsson and Willander 2009; Larsson et al. 2014).

Recognition memory is a subsystem of the declarative episodic memory referring to the ability to recognize a stimulus that was encountered in the past. It involves 2 different binding processes: recollection and familiarity (Tulving 1985; Wixted 2007). Recollection means remembering a stimulus and the context in which it was encoded, a process related to hippocampal activity. Familiarity involves remembering having encountered a stimulus without its contextual details, a process mainly related to extrahippocampal and perirhinal activity (Yonelinas 2002; Yonelinas et al. 2005; Bird 2017).

Evidence is scarce regarding neural basis of laboratory-based old/new ORM tasks, and few studies have shown that piriform cortex, amygdala, entorhinal cortex, hippocampus, thalamus, insula, and orbitofrontal cortex are involved in this mental process (Savic et al. 2000; Dade et al. 2002; Royet et al. 2011; Meunier et al. 2014). Furthermore, to the best of our knowledge only 1 study applied functional connectivity analysis using a general linear model (GLM) approach on empirically derived regions of interest (ROI) (Royet et al. 2011; Meunier et al. 2014). Importantly, GLM-based approaches have some limitations, especially regarding understudied research areas that require more explorative approach. Compared with other data-driven methods, such as independent component analysis (ICA), GLM approaches are less effective in noise-filtering and less sensitive in detecting brain networks (Xu et al. 2013).

Against this background, the aim of this study was to explore neural networks and correlates associated with 3 odor functions: passive smelling (PS), odor encoding (OE), and in

Editorial Decision 24 January 2023.

particular odor recognition memory (ORM). For the latter purpose, we used the odor recognition task from the validated test of episodic odor memory (Sniffin' TOM). The odors included in the Sniffin' TOM are common everyday odors, highly associable, and may therefore entail a recognition based more on recollection than familiarity (Larsson et al. 2006; Croy et al. 2015; Oleszkiewicz et al. 2019). Three analyses were performed on the functional magnetic resonance imaging (fMRI) data. First, ICA was applied for the whole brain in order to detect as many engaged brain networks as possible for each function. Second, a GLM analysis was employed to contrast different conditions both within and between sessions. Third, we performed an ROI analysis in order to investigate potential differences in memory responses during the ORM task. ROIs were selected based on the obtained ICA and GLM outcomes, as well as on previous studies investigating neural activity using old/new recognition paradigms (Kim 2013; Saive et al. 2014). More specifically, potential differences in signal change within insula, thalamus, middle frontal gyrus, posterior cingulate gyrus, precuneus, amygdala, posterior piriform cortex, and superior dentate gyrus were examined.

Materials and methods

Participants

A total of 26 healthy participants (16 females) with a mean age of 53 years (SD ±9.22) were recruited through advertisements at the University Hospital of Linköping. Participants reporting active colds or allergies, history of previous surgery in the nasal cavity, neurological disorders, psychiatric disorders, cognitive impairment, COVID-19 infection, mandibular implants, smoking, or magnetic/electromagnetic implants (such as pacemakers) were excluded. One participant did not complete the ORM session and was therefore excluded from the statistical analysis of this condition, yielding a sample of 25 participants (15 females, mean age 53 years, SD ±9.35). Written informed consent was obtained from all participants. The study was conducted in accordance with the 1964 Helsinki declaration and its later amendments and was approved by the Swedish Ethical Review Authority (registration number 2019-02679).

Odor stimulation design

The fMRI experiment consisted of 3 different olfactory sessions conducted on the same day, 1 session for each function: PS, OE, and ORM. A block design was employed across all sessions including everyday odors that were familiar and therefore easily associable (Hummel et al. 1997). In PS, 2 different odors, vanilla and peach, were presented in a pseudorandomized order. Participants were instructed to breath regularly and to inhale the presented odors. Participants were unaware of how many different odors would be presented and for how long. High cognitive demand was not required during this session leading to a short stimulation length of 4 s, followed by 20 s of passive resting period with odorless air. After this session, all participants verified that they could successfully perceive different odors indicating an intact sense of smell. In the OE session, 8 new odors from the Sniffin' TOM were presented in the following order: orange, banana, leather, cinnamon, turpentine, lemon, licorice, and garlic. Here, participants were instructed that they do not need to identify the presented odors but to memorize them. Stimulation length was 5 s, followed by 28 s of resting period with odorless air. Participants were asked to evaluate whether they detected an odor by finger tapping (index = yes, middle finger = no) after each odor presentation. The response window lasted for 10 s, starting 3 s after odor stimulation. Ten minutes after the conclusion of the OE session, the ORM session was initiated and included 16 odors: 8 target/old and 8 distractor/new odors presented in the following order: licorice, pineapple, orange, banana, rose, apple, cinnamon, anise, fish, coffee, leather, clove, peppermint, lemon, garlic, and turpentine. As in the OE session, stimulation length was 5 s, followed by a 28 s of resting period with odorless air. For each odor presented, the participant was instructed to decide whether an odor was "old" or "new" by finger tapping (index = "old," middle finger = "new"). Participants were thoroughly informed through goggles (visual cueing) regarding the different segments of each session (odor stimulation, response, and rest). All odors were delivered simultaneously to both nostrils, using the OG001 Multistimulator (Burghart Messtechnik GmbH, Wedel, Germany), embedded in medical air stream (2.5 L airflow per nostril), through Teflon-tubing (4 mm inner diameter). To remove residual odorants, a constant, inverse airflow was maintained inside the magnet aperture. All participants were instructed to breathe normally through the nose and to avoid sniffing that can influence the BOLD-signal (Sobel et al. 1998). All odors derived from the Sniffin' Sticks testing battery (Burghart Messtechnik GmbH, Wedel, Germany). A schematic representation of the olfactory stimulation and visual cueing is summarized in Fig. 1.

MRI image acquisition

MRI was performed with a 3T scanner (Siemens MAGNETOM Prisma, Siemens AG, Erlangen, Germany) using a 20-channel head-neck coil. We used a multiplex echo planar imaging (EPI) sequence, including an initial fat saturation pulse: repetition/echo time = 878/24 ms; flip angle = 56°; integrated parallel acquisition technique = 3; EPI factor = 68; field of view = 204 × 204 mm^2; # slices = 45; slice thickness (gap) = 3 (0) mm; voxel = 3 × 3 × 3 mm^3. For PS, 403 time points were collected (total scan time = 353.83 s). For OE, 320 time points were collected (total scan time = 280.96 s). For ORM, 620 time points were collected (total scan time = 544.36 s). Prior to fMRI acquisition, field mapping was performed with 2 different echo times (4.92 and 7.38 ms), in order to create a phase map. Additionally, high-resolution 3D T1-weighted structural scans were acquired in all participants. T1-weighted images were later co-registered with the functional images.

Independent component analysis

Tensorial ICA was carried out with MELODIC version 3.15, part of FSL 6.0 (FMRIB Analysis Group, University of Oxford, UK). Tensorial ICA allows a model-free decomposition of the variance in the signal, into different activation and artifactual components, including their spatial maps and time courses (Beckmann and Smith 2005). The following data preprocessing was applied to the input data: masking of non-brain voxels; voxel-wise demeaning of the data; normalization of the voxel-wise variance; preprocessed data

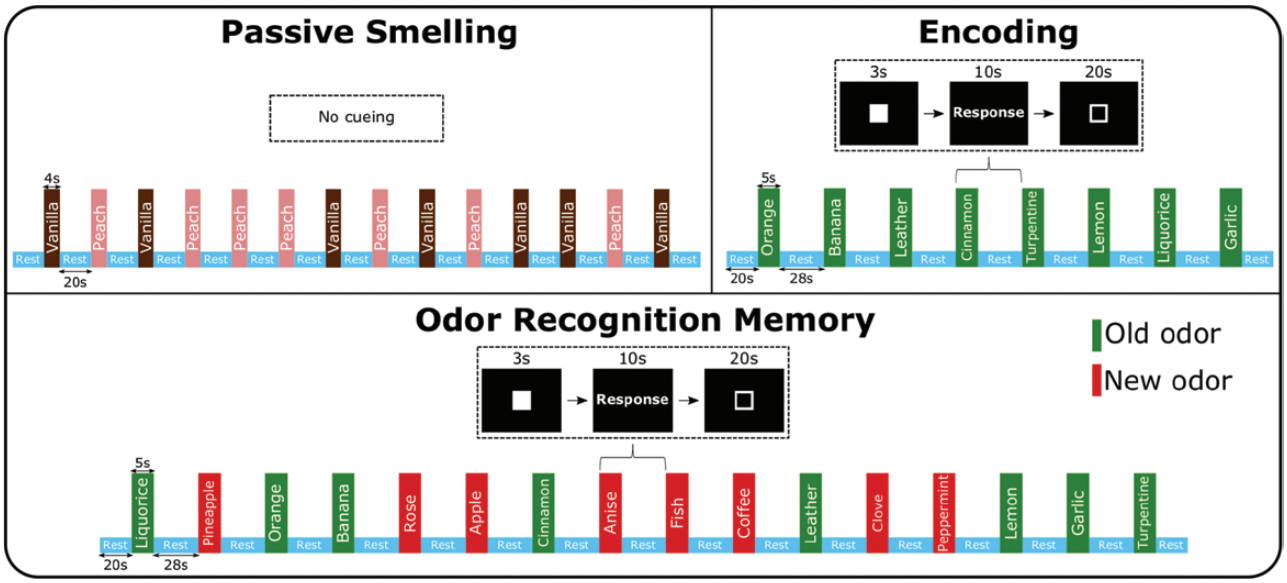

Fig. 1. Schematic representation of fMRI paradigm. Olfactory stimulation was performed in blocks for all 3 sessions: PS, OE, and ORM. Visual cueing was only used during OE and ORM.

were whitened and projected into a 25-dimensional subspace using Principal Component Analysis. The whitened observations were decomposed into sets of vectors that describe signal variation across the temporal domain (time courses), the session/subject domain and across the spatial domain (maps) by optimizing for non-Gaussian spatial source distributions using a fixed-point iteration technique (Hyvarinen 1999). Estimated component maps were divided by the SD of the residual noise and thresholded by fitting a mixture model to the histogram of intensity values (Beckmann and Smith 2004). In accordance with previous studies, we started with decomposing the signal into 20 components which subsequently increased to 25 (Hu et al. 2019). The 25 components analysis is presented in this study since it generated similar but slightly clearer results. Each independent component consists of a thresholded spatial map and a time course (temporal mode).

GLM analysis

GLM analysis was carried out with SPM12 (Wellcome Trust Centre for Neuroimaging, University College London, London, UK). Prior to preprocessing, the phase map of each participant was created using the default pipeline. Thereafter, all participants' images were separately realigned and the translation and rotation correction parameters were individually examined to ensure that no participant had significant head motion greater than 1 voxel in any direction. No participants were excluded due to head motion. Spatial normalization into Montreal Neurological Institute (MNI) space was initially performed on the anatomical T1-weighted image of each participant, and these normalization parameters were then applied to each respective functional image set. The normalized images were smoothed with an 8 mm full width half maximum Gaussian kernel. For PS, both odors combined were modeled as regressor of interest. For OE, detected and undetected odors were modeled separately as regressors of interest. For ORM, 4 responses; hit (Hit, odors correctly recognized as old), correct rejection (CR, odors correctly recognized as new), false alarm (FA, odors incorrectly recognized as old), and miss (Miss, odors incorrectly recognized as new) were modeled separately as regressors of interest. The resting periods were not explicitly modeled, while no-responses were modeled. The 6 motion parameters derived from the realignment step were included as covariates of no interest. At second level analysis, an ANOVA was performed contrasting first the conditions within every session: (i) detected and undetected odors from OE; (ii) Hit, CR, FA, and Miss from ORM. Subsequently, based on previous studies that demonstrated a hierarchy and interdependency in olfactory processing, we decided to perform the following contrasts in order to investigate distinct brain activities for ORM and Hit-responses: (i) Hit, CR, FA, and Miss from ORM and a combination of PS and OE; (ii) Hit from ORM and the combination of PS and detected odors from OE (Savic et al. 2000; Boesveldt et al. 2009).

ROI analysis

To further explore potential differences in the hemodynamic response signal during the 4 different response categories of ORM, we carried out ROI analysis with the MarsBaR 0.45 toolbox for SPM. To avoid circular reasoning, we designed our ROIs based on their anatomical location, instead of choosing voxels with significant activity from the GLM analysis. As most of these ROIs are anatomically large and/or complex, which could potentially mitigate measured signal change, we chose to draw spherical ROIs near the epicenter of the anatomical ROI. For this purpose, an experienced neuroradiologist (CG), blinded to the results of GLM, designed 16 spherical ROIs with the following coordinates (x, y, z in MNI space): left anterior insula (−36, 12, −2, radius 5 mm), right anterior insula (40, 16, 0, radius 5 mm), left medial dorsal thalamus (−6, −16, 8, radius 5 mm), right medial dorsal thalamus (8, −18, 6, radius 5 mm), left middle frontal gyrus (−40, 20, 38, radius 8 mm), right middle frontal gyrus (40, 20, 38, radius 8 mm), left posterior cingulate gyrus (−6, −42, 36, radius 7 mm), right posterior cingulate gyrus (8, −42, 36, radius 7 mm), left precuneus (−4, −74, 46, radius 6 mm), right precuneus (8, −72, 42, radius 6 mm), left dentate

gyrus of hippocampus (−16, −38, 4, radius 3 mm), right dentate gyrus of hippocampus (14, −38, 4, radius 3 mm), left amygdala (−23, −4, −18, radius 5 mm), right amygdala (23, −3, −18, radius 5 mm), left posterior piriform cortex (−24, 1, −17, radius 3 mm), and right posterior piriform cortex (24, 1, −17, radius 3 mm). We focused on ROIs with a direct relation to olfaction or an established role in memory. ROIs were designed on FSLeyes 1.0.13, using a standard MNI template with 2 mm slice thickness and are illustrated in Fig. 2. Thereafter, the finite impulse response (FIR) event time courses for each response within each ROI were plotted and peak signal change was identified for further statistical analysis.

Statistics

The Hit-rate (H) and FA-rate (F) in ORM were calculated and corrected as:

$$H = [(\text{Hit} + 0.5)/(N_1 + 1)], \quad F = [(\text{FA} + 0.5)/(N_2 + 1)]$$

N_1 represents the number of old odors and N_2 represents the number of new odors in the ORM session (Snodgrass and Corwin 1988; Royet et al. 2011). Thereafter, the discrimination score d' and the bias score c were computed as in accordance with signal detection theory (Macmillan and Creelman 2005):

$$d' = z(H)z(F), \quad c = -0.5[z(H) + z(F)]$$

The relationship between performance in the olfactory tasks and age was examined with Pearson's correlation coefficient test and difference between sexes was investigated with a 2-sample t-test assuming unequal variance. These computations were performed with R (R Development Core Team 2010).

The default threshold level of $P > 0.5$ was used for tensorial ICA in order to test the alternative hypothesis post statistically. To examine differences between components and their meaning, time to peak and reaction times were extracted and used in post hoc 2-sample t-test assuming unequal variance and Pearson's correlation. These computations were performed with R, and the results presented with mean, SDs, correlation coefficient (r), and P values (R Development Core Team 2010).

For the GLM analysis, whole brain analysis was assessed at $P < 0.05$ after family-wise error correction. The FIR event-related time courses represent percentage of signal change by time. Repeated measures ANOVA with Bonferroni correction for pairwise comparisons was employed separately for each ROI in order to estimate potential differences in peak signal change among Hit-, CR-, FA-, and Miss-responses. Statistical significance for ROI analysis was set at $P < 0.05$. Statistical analysis of the FIR event-related time courses was performed with IBM SPSS Statistics version 28.

Results

Behavioral data

Correlation analysis showed no significant correlation between age and performance in the different olfactory tasks ($P > 0.20$). Similarly, 2-sample t-tests assuming unequal variance showed no differences between sex. During PS (n = 26), all participants verified detection of odors. At OE (n = 26), participants detected 79% (SD = ±24%) of the 8 target odors and the mean reaction time was 2,730.92 ms (SD = ±487.07 ms). In the ORM session (n = 25), participants showed corrected Hit-rate of 68% (SD = ±18%) and corrected FA-rate of 41% (SD = ±16%), and the mean reaction time was 3,202.09 ms (SD = ±518.39 ms). More detailed information about the distribution of memory responses is shown in Table 1. Participants corrected Hit and FA rates were transformed into d' scores (M = 0.79, SD = ±0.70) indicating a detectable signal and varied discriminability. The bias score c (M = −0.15, SD = ±0.38) implied that the group showed a liberal response style and had a slightly stronger tendency to recognize odors as "old" (Lockhart and Murdock 1970; Snodgrass and Corwin 1988; Macmillan and Creelman 2005).

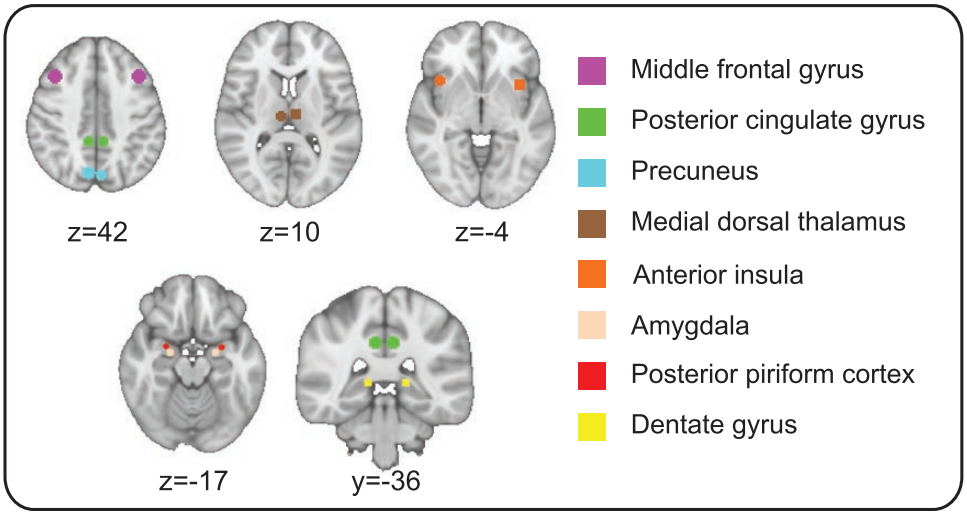

Fig. 2. Spatial representation of ROIs included in the post hoc ROI analysis. The following ROIs: anterior insula, medial dorsal thalamus, middle frontal gyrus, posterior cingulate gyrus, precuneus, dentate gyrus of hippocampus, amygdala, and posterior piriform cortex were extracted bilaterally, generating 16 ROIs in total.

Independent component analysis

ICA of PS revealed 1 independent component that was responsible for 3.12% of the explained signal variance (Fig. 3). The functional network of this component consisted of amygdala, part of the posterior piriform cortex, striatum, thalamus, insular cortex, and the secondary somatosensory cortex in both hemispheres, whereas its temporal profile coincided with the stimulation paradigm. A similar component, comprising olfactory cortex, insula, and basal ganglia was found for both OE and ORM (components #12 and #8, respectively, Figs. 4C and 5A).

ICA of OE revealed 2 additional relevant components: (i) 1 comprising hippocampus, ventral striatum, and posterior cingulate gyrus, and (ii) 1 comprising the prefrontal cortex and the medial part of thalamus in both hemispheres (components #10 and #11, respectively, Fig. 4A and B). Both components coincided temporally with odor stimulation. ICA of ORM revealed a primarily limbic component, comprising hippocampus and posterior cingulate gyrus in both hemispheres (component #11, Fig. 5B). As opposed to the aforementioned components, the temporal representation of the latter one was dissociated from the stimulation paradigm, with triggering occurring during rest.

Table 1. Descriptive data of behavioral results in OE and ORM.

Memory process	Response type	Proportion (SD)	Minimum	Maximum
Encoding	Detected	0.79 (0.24)	2	8
	Undetected	0.21 (0.24)	0	6
Retrieval	Hit	0.68 (0.18)	2	8
	Miss	0.32 (0.18)	0	6
	CR	0.59 (0.16)	2	7
	FA	0.41 (0.16)	1	6

Post hoc 2-sample *t*-tests assuming unequal variation revealed that the mean time to peak in ORM component #11 (M = 37.05 s, SD = ±0.52 s) was significantly longer compared with PS component #10 (M = 6.59 s, SD = ±1.43 s, $P < 0.001$) and OE component #10 (M = 13.32 s, SD = ±1.05 s, $P < 0.001$). In attempt to investigate the meaning of this delayed triggering, we performed several post hoc correlations and *t*-tests assuming unequal variance. No significant correlations were found between the overall time to peak in ORM component #11 and proportion of correct responses, proportion of incorrect responses, and reaction times. When examined old and new odors separately, some tendencies were observed. The reaction time in relation to new odors (M = 3,435.91 ms, SD = ±440.24 ms) tended to be longer (P = 0.06) than in relation to old odors (M = 2,934.86 ms, SD = ±494.69 ms). Accordingly, time to peak and reaction time tended to correlate only concerning new odors (r = 0.64, P = 0.08).

General linear model

When contrasting the ORM session against the combination of OE and PS (ORM > OE and PS), we found significantly higher activation within anterior insula, pallidum, and thalamus bilaterally, parts of hippocampus, as well as the middle frontal gyrus and the supplementary motor area bilaterally (Fig. 6A). When comparing Hit-responses from ORM to the combination of PS and detected odors during OE (Hit < PS and detected in OE), we found significantly lower activation within amygdala and piriform cortex bilaterally, parts of insula and thalamus, as well as the inferior parietal lobule (Fig. 6B). Contrasts with the opposite directions as well as contrasts within OE (detected vs. undetected odors) and within ORM (all possible combinations of Hit, CR, FA, and Miss) did not demonstrate significant results.

ROI analysis

Peak signal change across all 4 responses of ORM (Hit, CR, FA, and Miss) was identified with the FIR event time course function of the marsbar toolbox, within 8 ROIs in each

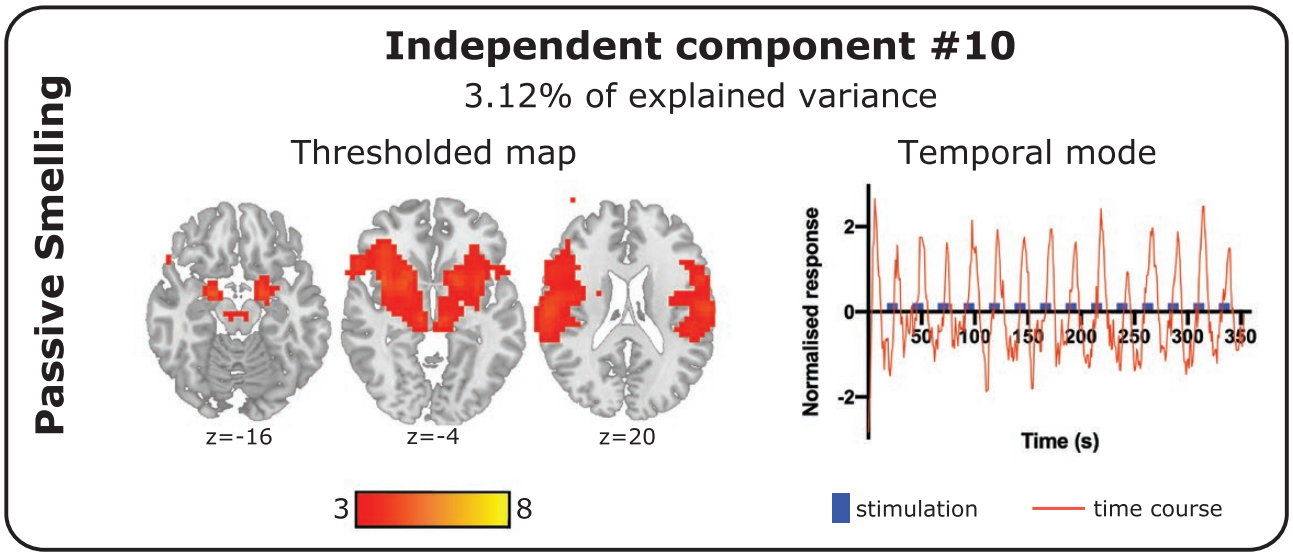

Fig. 3. Results from ICA of PS. One independent component was associated with functional connectivity among parts of amygdala and posterior piriform cortex (z = −16), basal ganglia, thalamus, and insula (z = −4), as well as the secondary somatosensory cortex (z = 20). The signal change for this network (temporal mode) coincided with olfactory stimulation. The default threshold of P > 0.5 was used for testing the alternative hypothesis post statistically. Color bars are given in terms of *T*-statistic. Left and right in radiological convention.

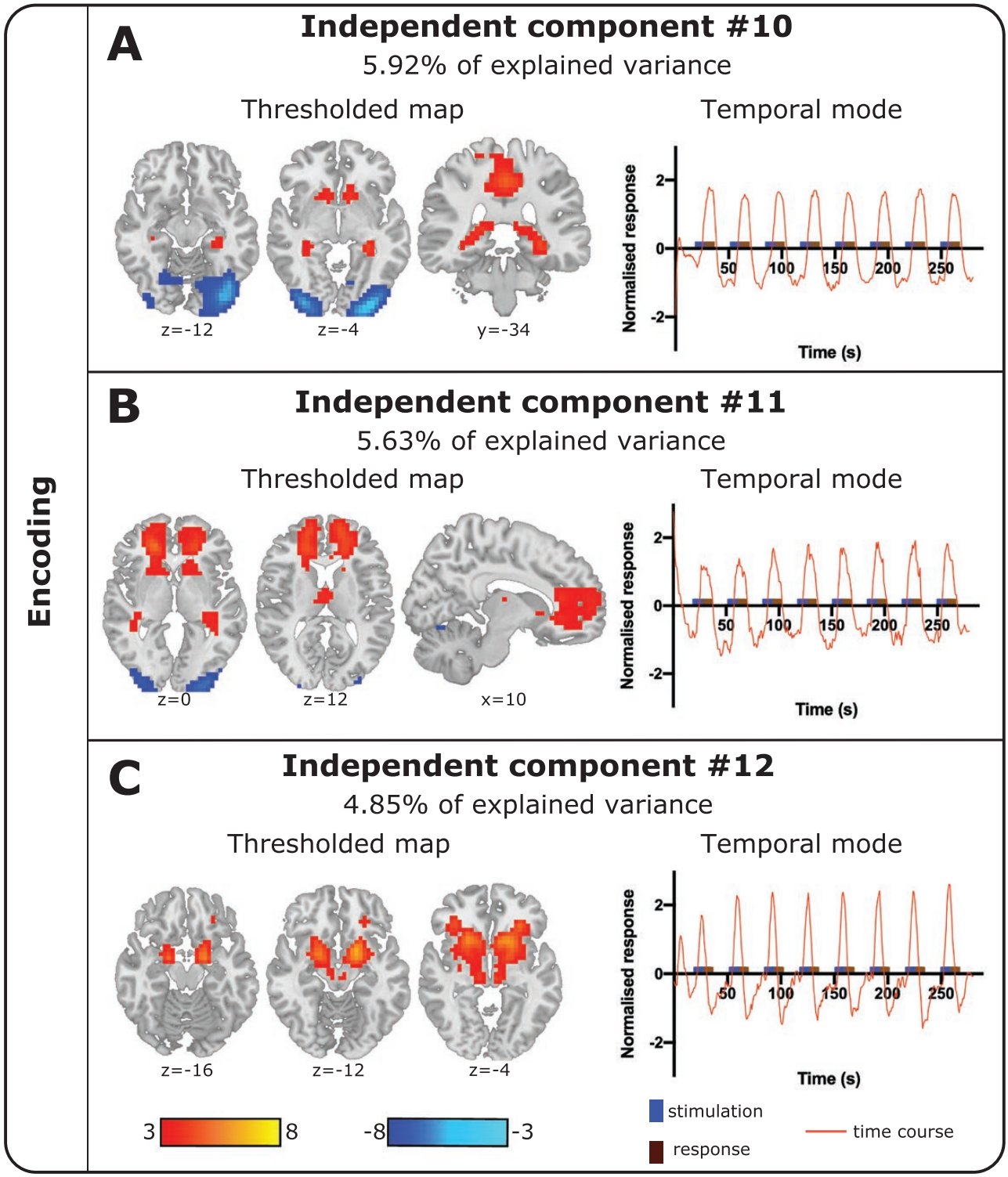

Fig. 4. Results from ICA of OE. A) Independent component #10 was associated with functional connectivity among hippocampus ($z = -12$, $y = -34$), ventral striatum ($z = -4$), and posterior cingulate gyrus ($y = -34$). B) Another component (#11) was associated with functional connectivity among caudate nucleus ($z = 0$), the medial part of thalamus ($z = 12$), and the prefrontal cortex ($z = 0$, $z = 12$, $x = 10$). C) Independent component #12 was associated with functional connectivity among amygdala and posterior piriform cortex ($z = -16$, $z = -12$), as well as basal ganglia, thalamus, and anterior insula ($z = -4$). The signal change for all these networks (temporal mode) coincided with olfactory stimulation. The default threshold of $P > 0.5$ was used for testing the alternative hypothesis post statistically. Color bars are given in terms of *T*-statistic. Left and right in radiological convention.

brain hemisphere. A repeated measures ANOVA with pairwise comparisons and Bonferroni correction revealed significantly lower peak signal change for Hit-responses compared with FA in anterior insula, posterior cingulate gyrus, dentate gyrus, amygdala, and posterior piriform cortex bilaterally. In addition, Hit-responses showed significantly lower peak signal change than CR in posterior cingulate gyrus and amygdala bilaterally, left middle frontal gyrus and left posterior

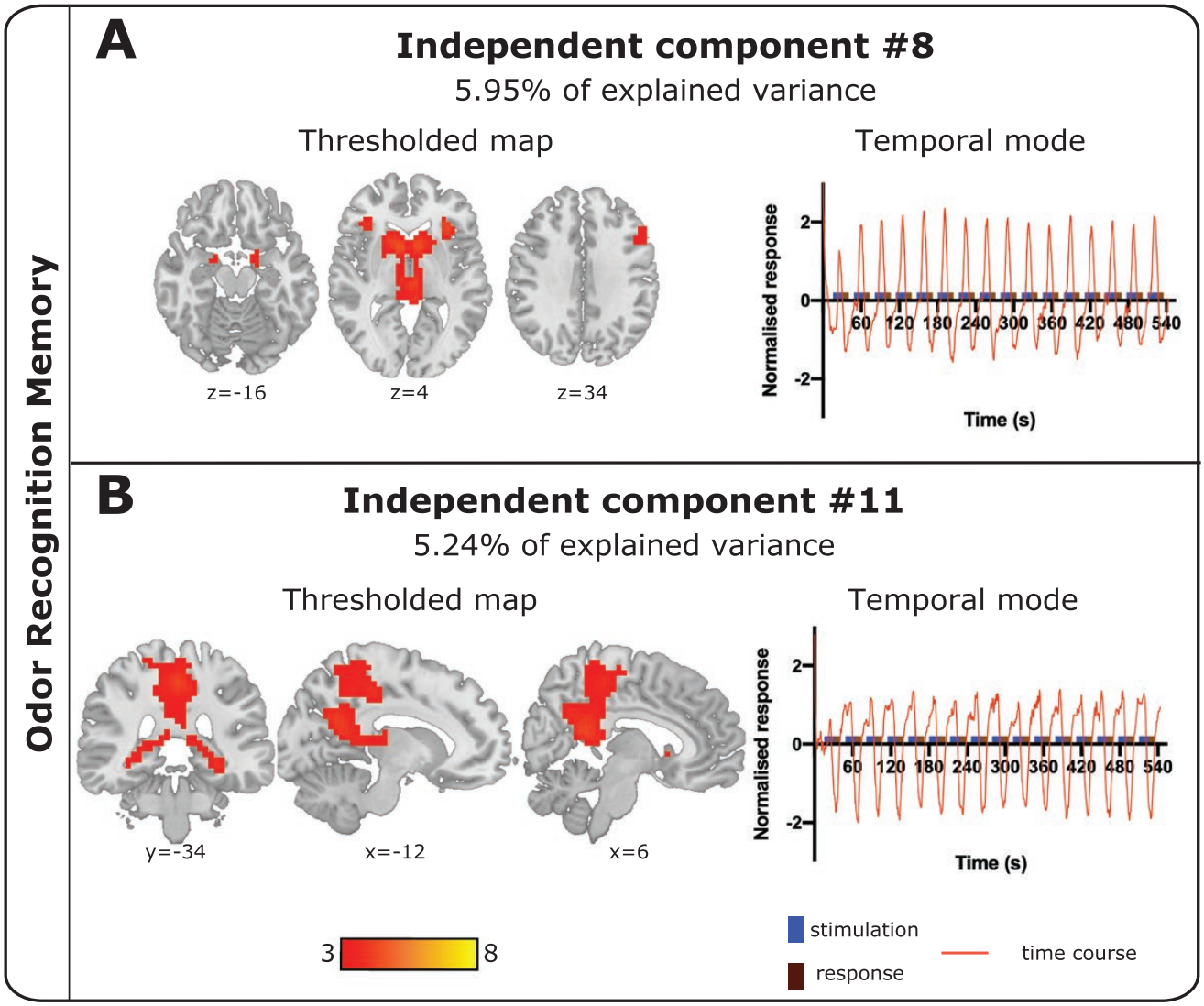

Fig. 5. Results from ICA of ORM. A) Independent component #8 was associated with functional connectivity among amygdala and posterior piriform cortex ($z = -16$), basal ganglia, thalamus, and anterior insula ($z = 4$), as well the left middle frontal gyrus ($z = 34$). The signal change for this network (temporal mode) coincided with olfactory stimulation. B) Another component (#11) was associated with functional connectivity among hippocampus ($y = -34$), as well as posterior cingulate gyrus and precuneus ($x = -12$, $x = 6$). Signal change for this network is dissociated with stimulation, with positive signal change occurring during the resting time. The default threshold of $P > 0.5$ was used for testing the alternative hypothesis post statistically. Color bars are given in terms of *T*-statistic. Left and right in radiological convention.

piriform cortex. Hit-responses showed significantly lower peak signal change than Miss in posterior cingulate gyrus bilaterally. CR showed significantly lower peak signal change than FA in left posterior piriform cortex. We did not find any significant pairwise differences in thalamus, precuneus, or right middle frontal gyrus. The ANOVA results including pairwise comparisons are presented in detail at Table 2 and Fig. 7.

Discussion

The aim of this study was to explore the neural networks and correlates associated with 3 olfactory functions: PS, OE, and ORM. Corroborating previous work, the ICA suggested a parallel and hierarchical model where functional connectivity networks including amygdala, piriform cortex, basal ganglia, and insula were associated with both lower- (PS) and higher-order (OE and ORM) olfactory functions. Nevertheless, the present study slightly differed from previous findings by demonstrating mainly a bilateral brain activity without any obvious right hemisphere lateralization and by showing that the piriform cortex played a key role across all 3 odor functions (Savic et al. 2000; Dade et al. 2002; Royet and Plailly 2004; Royet et al. 2011; Meunier et al. 2014; Saive et al. 2014). During OE and ORM, the functional networks expanded toward hippocampus, posterior cingulate gyrus, and frontal brain areas indicating their general role in higher-order cognitive functions, and more specifically in the encoding and recollection rather than familiarity of episodic odor information. The similarity between the networks involved at OE and ORM indicated a neuronal reinstatement which in previous studies was related to memory storage (Frankland et al. 2019). Further, ORM engaged 2 additional regions: the precuneus and the left middle frontal gyrus. The former is related to the default-mode network and the process of ecphory i.e. reeexperiencing stimuli that were encountered in the past (Nyberg et al. 1995), while the left

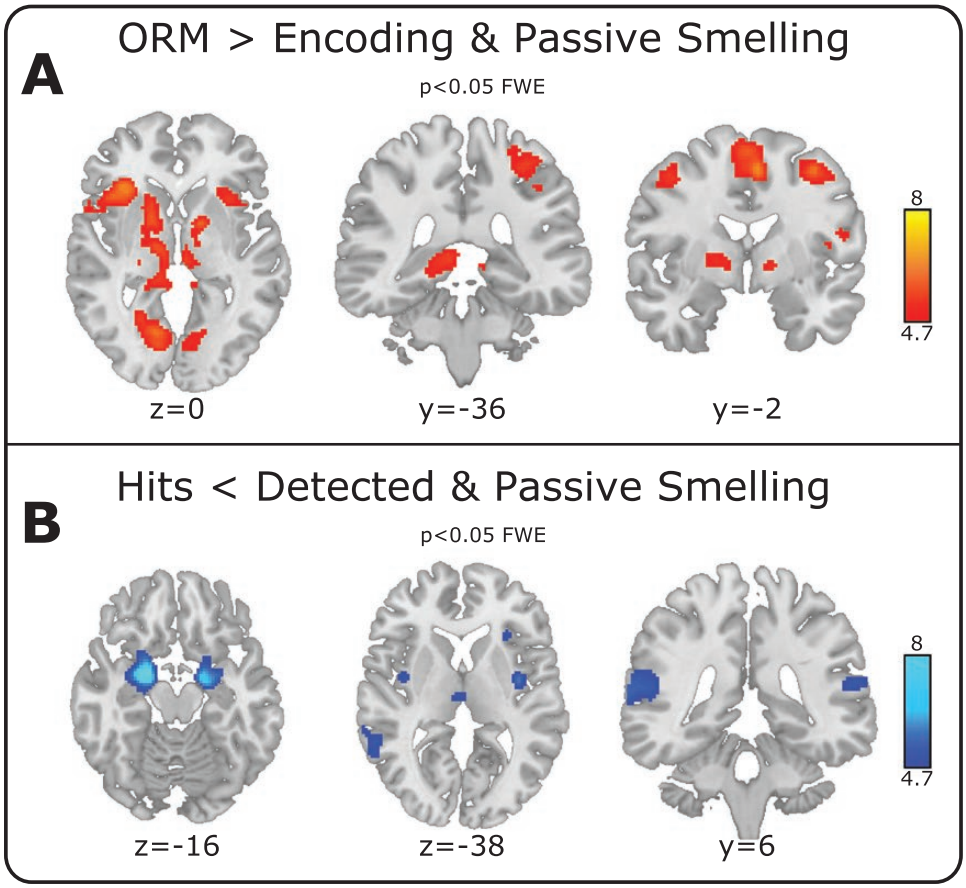

Fig. 6. Results from GLM analysis. A) During ORM, anterior insula, pallidum, and thalamus bilaterally ($z = 0$), parts of hippocampus, particularly on the right hemisphere ($y = -36$), as well as the middle frontal gyrus and the supplementary motor area bilaterally ($y = -2$) showed significantly higher activation compared with the combination of PS and OE. B) For Hit during ORM, amygdala and piriform cortex bilaterally ($z = -16$), parts of insula (mostly posteriorly), and thalamus ($z = -38$), as well as the inferior parietal lobule ($y = -38$) showed significantly lower activation compared with the combination of PS and perceived odors during OE. Left and right in radiological convention; $P < 0.05$ family-wise error (FWE) corrected.

middle frontal gyrus which is associated with decision-making and more complex episodic memory tasks (Nolde et al. 1998; Cabeza and Nyberg 2000; Renoult et al. 2019).

Intriguingly, although some differences between OE and ORM regarding brain functional networks were observed, the main difference was related to temporal representation. Only in ORM were hippocampus and posterior cingulate gyrus dissociated from odor stimulation and recognition. To the best of our knowledge, this is the first study demonstrating such evidence in olfaction. The delayed triggering may be associated with task difficulty and strategic retrieval processes i.e. mental procedures used in order to complete a demanding retrieval task which precedes ecphory (Wilson and Stevenson 2006; Gonthier 2020). Nevertheless, the significantly longer time to peak in this component showed greater tendency to be related to new odors (odor novelty). Only in new odors reaction times showed tendency to be related to time to peak. In light of these indications and previous studies, it is more likely that the delayed triggering of the hippocampus and posterior cingulate is related to a postrecognition incidental encoding of new odors (Staresina et al. 2012). This hypothesis requires further investigation in future studies since this process was not adequately controlled in our study and the abovementioned indications did not reach significance level.

The GLM analysis demonstrated a significant higher activity at ORM compared with a combination of PS and OE within the anterior insula, globus pallidus, and thalamus, parts of hippocampus, as well as the middle frontal gyrus excluding the precuneus demonstrated by ICA. This is in accordance with few previous studies, indicating that ICA is more sensitive in detecting the involvement of different brain regions and therefore should be applied as an explorative complement to GLM, especially regarding understudied research areas (Xu et al. 2013; Georgiopoulos et al. 2019). Interestingly, by contrasting only Hit-responses with a combination of PS and detected odors during OE, we found an opposite activation pattern, with significantly lower activity in amygdala, piriform cortex, parts of insula, thalamus, and the inferior parietal lobule. This observation indicates that the significant high brain activity at ORM was more related to other cognitive and retrieval processes than the successful retrieval of episodic odor information, i.e. Hit-responses.

To further distinguish Hit-rates from the other recognition responses, we performed an ROI analysis focusing on signal change. The results corresponded with the GLM outcomes demonstrating a significantly lower peak signal change in most of the selected ROIs at Hit-responses, namely insula, dentate gyrus, amygdala, posterior piriform cortex, posterior cingulate gyrus bilaterally as well as left middle frontal gyrus. Both the observed lower brain activity and the lower peak signal change at Hit-responses are in line with the concept of neural response suppression related to familiarity i.e. deactivations of

Table 2. Repeated measures ANOVA for peak signal change within 8 ROIs, for each response type during the ORM fMRI session.

ROI		Hit[a]	CR[a]	FA[a]	Miss[a]	Sphericity (Mauchly's test)	Greenhouse–Geisser Epsilon (ε)[b]	Within-subjects effects[c]	Significant pairwise comparisons[d]
Anterior insula	Right	0.908 ± 0.047	1.05 ± 0.069	1.183 ± 0.093	1.029 ± 0.085	$P = 0.259$	Sphericity assumed	$P = 0.004$*	Hit vs. FA ($P = 0.006$)
	Left	0.663 ± 0.038	0.804 ± 0.071	0.949 ± 0.094	0.802 ± 0.1	$P = 0.467$	Sphericity assumed	$P = 0.001$*	Hit vs. FA ($P = 0.004$)
Medial dorsal thalamus	Right	0.8 ± 0.04	0.857 ± 0.077	0.91 ± 0.07	0.908 ± 0.074	$P = 0.725$	Sphericity assumed	$P = 0.210$	—
	Left	0.892 ± 0.041	0.999 ± 0.075	1.096 ± 0.08	1.055 ± 0.068	$P = 0.739$	Sphericity assumed	$P = 0.071$	—
Middle frontal gyrus	Right	0.546 ± 0.037	0.62 ± 0.061	0.664 ± 0.08	0.65 ± 0.066	$P = 0.190$	Sphericity assumed	$P = 0.077$	—
	Left	0.466 ± 0.043	0.612 ± 0.082	0.667 ± 0.106	0.628 ± 0.099	$P = 0.002$	$\varepsilon = 0.732$	$P = 0.021$*	Hit vs. CR ($P = 0.037$)
Posterior cingulate gyrus	Right	0.253 ± 0.017	0.4 ± 0.033	0.412 ± 0.039	0.42 ± 0.047	$P = 0.217$	Sphericity assumed	$P < 0.001$*	Hit vs. CR ($P = 0.002$) Hit vs. FA ($P = 0.006$) Hit vs. Miss ($P = 0.034$)
	Left	0.316 ± 0.24	0.474 ± 0.37	0.471 ± 0.42	0.499 ± 0.54	$P = 0.1$	Sphericity assumed	$P < 0.001$*	Hit vs. CR ($P = 0.006$) Hit vs. FA ($P = 0.018$) Hit vs. Miss ($P = 0.04$)
Precuneus	Right	1.047 ± 0.069	1.177 ± 0.081	1.184 ± 0.077	1.263 ± 0.105	$P = 0.036$	0.755	$P = 0.083$	—
	Left	1.504 ± 0.134	1.639 ± 0.137	1.710 ± 0.157	1.731 ± 0.146	$P = 0.001$	0.693	$P = 0.278$	—
Dentate gyrus	Right	0.581 ± 0.051	0.687 ± 0.048	0.805 ± 0.079	0.742 ± 0.084	$P = 0.085$	Sphericity assumed	$P = 0.016$*	Hit vs. FA ($P = 0.005$)
	Left	0.454 ± 0.027	0.541 ± 0.031	0.644 ± 0.05	0.63 ± 0.064	$P = 0.043$	0.752	$P = 0.021$*	Hit vs. FA ($P = 0.008$)
Amygdala	Right	0.892 ± 0.035	1.18 ± 0.058	1.303 ± 0.069	1.145 ± 0.128	$P = 0.001$	0.620	$P = 0.007$*	Hit vs. CR ($P = 0.002$) Hit vs. FA ($P < 0.001$)
	Left	1.162 ± 0.052	1.584 ± 0.1	1.783 ± 0.116	1.363 ± 0.147	$P = 0.011$	0.720	$P < 0.001$*	Hit vs. CR ($P < 0.001$) Hit vs. FA ($P < 0.001$)
Posterior piriform cortex	Right	1.234 ± 0.057	1.365 ± 0.043	1.682 ± 0.094	1.777 ± 0.204	$P < 0.001$	0.554	$P = 0.018$*	Hit vs. FA ($P = 0.008$)
	Left	1.76 ± 0.07	2.488 ± 0.139	2.839 ± 0.182	2.217 ± 0.268	$P < 0.001$	0.609	$P < 0.001$*	Hit vs. CR ($P < 0.001$) Hit vs. FA ($P < 0.001$) CR vs. FA ($P = 0.014$)

[a]Mean value ± standard error.
[b]Epsilon presented only if sphericity is not assumed (Mauchly's test <0.05).
[c]If sphericity is not assumed, the Greenhouse–Geisser results are presented for $\varepsilon < 0.75$ and the Huynh–Feldt results are presented for $\varepsilon > 0.75$.
[d]Including Bonferroni correction. Only significant results are presented.
*Statistical significance.

brain regions due to repetitive exposure for the same stimuli and prior knowledge (Henson and Rugg 2003; Poppenk et al. 2016; de Chastelaine et al. 2017). Few previous studies have found that low brain activity is also associated with fluency, the ease to process a stimulus. This finding implies that future scientific research needs to investigate the differences between neural suppression related to successful retrieval versus fluency (Dew and Cabeza 2013). Furthermore, our findings suggests that the precuneus and thalamus have a general role in retrieval processes due to the nonsignificant signal peak change at Hit compared with other retrieval responses.

Some limitations of the present study should be highlighted. The study did not include breathing monitoring which might have influenced the measured BOLD-signal from the olfactory cortex (Sobel et al. 1998). Task difficulty and stimulus novelty might also have affected the results and therefore

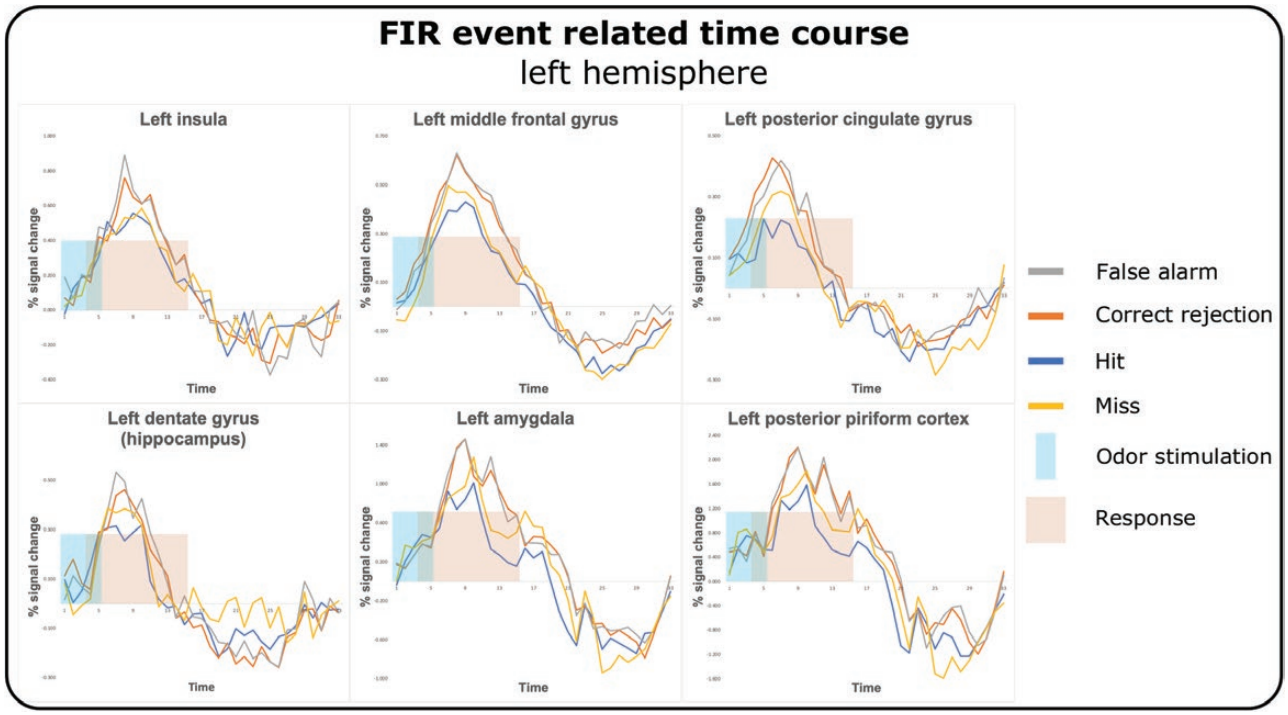

Fig. 7. FIR event-related time courses for anterior insula, middle frontal gyrus, posterior cingulate gyrus, dentate gyrus, amygdale, and posterior piriform cortex (left hemisphere) during the odor recollection memory task. For insula, posterior cingulate gyrus, dentate gyrus, amygdala, and posterior piriform cortex peak signal change of Hit was significantly lower than the one of FA (repeated measures ANOVA, Table 2). Additionally, peak signal change of Hit was significantly lower than the one of CR in middle frontal gyrus, posterior cingulate gyrus, amygdala, and posterior piriform cortex (repeated measures ANOVA, Table 2). Peak signal change of Hit was significantly lower than the one of Miss only in posterior cingulate gyrus (repeated measures ANOVA, Table 2).

should be mentioned here (Gould et al. 2003; Wittmann et al. 2007; de Chastelaine et al. 2017). However, the odors used in our paradigm were acquired from the validated ORM test Sniffin' TOM. The olfactory items included in this test demonstrated correspondence regarding familiarity level (Hummel et al. 1997; Croy et al. 2015). Furthermore, although the shorter odor presentation in PS compared with the other sessions minimized the risk for fatigue it might also have acted as a confounder. Our sample did not show any sex differences or influence of age in OE and ORM performance. Nevertheless, most of the scientific evidence demonstrates deterioration of olfactory and memory function with increasing age and a female superiority regarding olfactory performance (Doty and Kamath 2014; Croy et al. 2015; Sorokowska et al. 2020). This contradiction might be related to the small sample size, wide age range and fewer male participants. However, several different studies demonstrated in relation to other modalities than olfaction that familiarity effects were preserved with increasing age (de Chastelaine *et al.* 2017). These findings can be as well associated with the limited number of olfactory items included in the fMRI paradigm. Consequently, since the number of items in our paradigm was limited, each memory response category included few trials. However, a larger item set would have increased the difficulty level of the task which was already challenging (Engen and Ross 1973; Herz and Engen 1996). To further investigate these findings future studies may beneficially include breathing monitoring and larger sample sizes including various equally divided age and sex subpopulations, administering a larger odor item set, and compare performance in different odor item sets.

In summary, our findings show that low hemodynamic response and low peak signal change within insula and parts of the limbic system are associated with successful retrieval of episodic odor information (odor familiarity), indicating a relation between Hit-responses and neural response suppression. Additionally, a network including hippocampus and posterior cingulate is temporally dissociated from odor stimulation and recognition. Some indications imply that this network may be involved in a postrecognition incidental encoding process related to new odors (odor novelty), however further research is needed to clarify this hypothesis. Finally, the utilization of ICA, especially in explorative research studies, is very important since this type of analysis is more sensitive than standard GLM in detecting brain regions involved in different mental processes.

Funding

The study was supported by Linköping University Hospital Research Fund grant number RÖ-938229, Forskningsrådet i Sydöstra Sverige grant number FORSS-931891.

Acknowledgments

The authors would like to thank all the participants, medical personnel, research colleagues, and anonymous reviewers. All contributed greatly to this research.

Conflict of interest

None declared.

Data availability

The data included in this study will be available on reasonable request to the corresponding author.

References

Arshamian A, Iannilli E, Gerber JC, Willander J, Persson J, Seo HS, Hummel T, Larsson M. The functional neuroanatomy of odor evoked autobiographical memories cued by odors and words. *Neuropsychologia*. 2013;51(1):123–131.

Beckmann CF, Smith SM. Probabilistic independent component analysis for functional magnetic resonance imaging. *IEEE Trans Med Imaging*. 2004;23(2):137–152.

Beckmann CF, Smith SM. Tensorial extensions of independent component analysis for multisubject FMRI analysis. *Neuroimage*. 2005;25(1):294–311.

Bird CM. The role of the hippocampus in recognition memory. *Cortex*. 2017;93:155–165.

Boesveldt S, de Muinck Keizer RJ, Wolters E, Berendse HW. Odor recognition memory is not independently impaired in Parkinson's disease. *J Neural Transm*. 2009;116(5): 575–578.

Cabeza R, Nyberg L. Imaging cognition II: an empirical review of 275 PET and fMRI studies. *J Cogn Neurosci*. 2000;12(1):1–47.

Cornell Kärnekull S, Jönsson FU, Willander J, Sikström S, Larsson M. Long-term memory for odors: influences of familiarity and identification across 64 days. *Chem Senses*. 2015;40(4):259–267.

Croy I, Zehner C, Larsson M, Zucco GM, Hummel T. Test-retest reliability and validity of the Sniffin' TOM odor memory test. *Chem Senses*. 2015;40(3):173–179.

Dade LA, Zatorre RJ, Jones-Gotman M. Olfactory learning: convergent findings from lesion and brain imaging studies in humans. *Brain*. 2002;125(1):86–101.

de Chastelaine M, Mattson JT, Wang TH, Donley BE, Rugg MD. Independent contributions of fMRI familiarity and novelty effects to recognition memory and their stability across the adult lifespan. *Neuroimage*. 2017;156:340–351.

Dew ITZ, Cabeza R. A broader view of perirhinal function: from recognition memory to fluency-based decisions. *J Neurosci*. 2013;33(36):14466–14474.

Doty RL, Kamath V. The influences of age on olfaction: a review. *Front Psychol*. 2014;5:20.

Engen T, Ross BM. Long-term memory of odors with and without verbal descriptions. *Q J Exp Psychol*.1973;100(2):221–227.

Frankland PW, Josselyn SA, Köhler S. The neurobiological foundation of memory retrieval. *Nat Neurosci*. 2019;22(10):1576–1585.

Georgiopoulos C, Witt ST, Haller S, Dizdar N, Zachrisson H, Engström M, Larsson EM. A study of neural activity and functional connectivity within the olfactory brain network in Parkinson's disease. *Neuroimage Clin*. 2019;23:101946.

Gonthier C. Charting the diversity of strategic processes in visuospatial short-term memory. *Perspect Psychol Sci*. 2020;16(2):294–318.

Gould RL, Brown RG, Owen AM, ffytche DH, Howard RJ. fMRI BOLD response to increasing task difficulty during successful paired associates learning. *Neuroimage*. 2003;20(2):1006–1019.

Henson RNA, Rugg MD. Neural response suppression, haemodynamic repetition effects, and behavioural priming. *Neuropsychologia*. 2003;41(3):263–270.

Herz RS, Engen T. Odor memory: review and analysis. *Psychon Bull Rev*. 1996;3(3):300–313.

Hu G, Zhang Q, Waters AB, Li H, Zhang C, Wu J, Cong F, Nickerson LD. Tensor clustering on outer-product of coefficient and component matrices of independent component analysis for reliable functional magnetic resonance imaging data decomposition. *J Neurosci Methods*. 2019;325:108359.

Hummel T, Sekinger B, Wolf SR, Pauli E, Kobal G. 'Sniffin' sticks': olfactory performance assessed by the combined testing of odor identification, odor discrimination and olfactory threshold. *Chem Senses*. 1997;22(1):39–52.

Hyvarinen A. Fast and robust fixed-point algorithms for independent component analysis. *IEEE Trans Neural Netw*. 1999;10(3):626–634.

Kim H. Differential neural activity in the recognition of old versus new events: an activation likelihood estimation meta-analysis. *Hum Brain Mapp*. 2013;34(4):814–836.

Larsson M, Oberg C, Bäckman L. Recollective experience in odor recognition: influences of adult age and familiarity. *Psychol Res*. 2006;70(1):68–75.

Larsson M, Willander J. Autobiographical odor memory. *Ann N Y Acad Sci*. 2009;1170:318–323.

Larsson M, Willander J, Karlsson K, Arshamian A. Olfactory LOVER: behavioral and neural correlates of autobiographical odor memory. *Front Psychol*. 2014;5:1–5.

Lockhart RS, Murdock BB. Memory and the theory of signal detection. *Psychol Bull*. 1970;74(2):100–109.

Macmillan NA, Creelman CD. *Detection theory. a user's guide*. New York: Psychological Press; 2005.

Meunier D, Fonlupt P, Saive AL, Plailly J, Ravel N, Royet JP. Modular structure of functional networks in olfactory memory. *Neuroimage*. 2014;95:264–275.

Nolde SF, Johnson MK, Raye CL. The role of prefrontal cortex during tests of episodic memory. *Trends Cogn Sci*. 1998;2(10):399–406.

Nyberg L, Tulving E, Habib R, Nilsson LG, Kapur S, Houle S, Cabeza R, McIntosh AR. Functional brain maps of retrieval mode and recovery of episodic information. *Neuroreport*. 1995;7(1):249–252.

Oleszkiewicz A, Schriever VA, Croy I, Hähner A, Hummel T. Updated Sniffin' Sticks normative data based on an extended sample of 9139 subjects. *Eur Arch Otorhinolaryngol*. 2019;276(3):719–728.

Poppenk J, McIntosh AR, Moscovitch M. fMRI evidence of equivalent neural suppression by repetition and prior knowledge. *Neuropsychologia*. 2016;90:159–169.

R Development Core Team. *R: a language and environment for statistical computing*. Vienna (Austria): R Foundation for Statistical Computing; 2010.

Renoult L, Irish M, Moscovitch M, Rugg MD. From knowing to remembering: the semantic–episodic distinction. *Trends Cogn Sci*. 2019;23(12):1041–1057.

Royet JP, Morin-Audebrand L, Cerf-Ducastel B, Haase L, Issanchou S, Murphy C, Fonlupt P, Sulmont-Rosse C, Plailly J. True and false recognition memories of odors induce distinct neural signatures. *Front Hum Neurosci*. 2011;65:15. Article no.: 5.

Royet J-P, Plailly J. Lateralization of olfactory processes. *Chem Senses*. 2004;29:731–745.

Saive AL, Royet JP, Plailly J. A review on the neural bases of episodic odor memory: from laboratory-based to autobiographical approaches. *Front Behav Neurosci*. 2014;8:10. Article no.: 240.

Savic I, Gulyas B, Larsson M, Roland P. Olfactory functions are mediated by parallel and hierarchical processing. *Neuron*. 2000;26(3):735–745.

Snodgrass JG, Corwin J. Pragmatics of measuring recognition memory: applications to dementia and amnesia. *J Exp Psychol Gen*. 1988;117(1):34–50.

Sobel N, Prabhakaran V, Desmond JE, Glover GH, Goode RL, Sullivan EV, Gabrieli JD. Sniffing and smelling: separate subsystems in the human olfactory cortex. *Nature*. 1998;392(6673):282–286.

Sorokowska A, Sabiniewicz A, Larsson M. TOM-32-An extended test for the assessment of olfactory memory. *J Neurosci Methods*. 2020;344:108873.

Staresina BP, Fell J, Do Lam AT, Axmacher N, Henson RN. Memory signals are temporally dissociated in and across human hippocampus and perirhinal cortex. *Nat Neurosci*. 2012;15(8):1167–1173.

Tulving E. Memory and consciousness. *Can Psychol*. 1985;26(1):1–12.

Wilson DA, Stevenson RJ. *Learning to smell: olfactory perception from neurobiology to behavior*. Baltimore (MD): Johns Hopkins University Press; 2006.

Wittmann BC, Bunzeck N, Dolan RJ, Düzel E. Anticipation of novelty recruits reward system and hippocampus while promoting recollection. *Neuroimage*. 2007;38(1):194–202.

Wixted JT. Dual-process theory and signal-detection theory of recognition memory. *Psychol Rev*. 2007;114(1):152–176.
Xu J, Potenza M, Calhoun V. Spatial ICA reveals functional activity hidden from traditional fMRI GLM-based analyses. *Front Neurosci*. 2013;7:1–4.
Yonelinas AP. The nature of recollection and familiarity: a review of 30 years of research. *J Mem Lang*. 2002;46(3):441–517.
Yonelinas AP, Otten LJ, Shaw KN, Rugg MD. Separating the brain regions involved in recollection and familiarity in recognition memory. *J Neurosci*. 2005;25(11):3002–3008.
Zhou G, Olofsson JK, Koubeissi MZ, Menelaou G, Rosenow J, Schuele SU, Xu P, Voss JL, Lane G, Zelano C. Human hippocampal connectivity is stronger in olfaction than other sensory systems. *Prog Neurobiol*. 2021;201:102027.